Characterization of the High-Spin Heme *x* in the Cytochrome b_6f Complex of Oxygenic Photosynthesis[†]

Huamin Zhang,*[,‡] Andrew Primak,[§] John Cape,[||] Michael K. Bowman,[§,||] David M. Kramer,[||] and William A. Cramer*[,‡]

Department of Biological Sciences, Lilly Hall of Life Sciences, Purdue University, West Lafayette, Indiana 47907-2054, Structural Biology and Microimaging, Battelle Northwest Laboratory, P.O. Box 999 K8-98, Richland, Washington 99352-0999, and Institute of Biological Chemistry, Washington State University, 289 Clark Hall, Pullman, Washington 99164-6340

Received July 30, 2004; Revised Manuscript Received October 1, 2004

ABSTRACT: X-ray structures at 3.0−3.1 Å resolution of the cytochrome b_6f complex from the cyanobacterium *Mastigocladus laminosus* [Kurisu, G., Zhang, H., Smith, J. L., and Cramer, W. A. (2003) *Science 302*, 1009−1014] and the green alga *Chlamydomonas reinhardtii* [Stroebel, D., Choquet, Y., Popot, J.-L., and Picot, D. (2003) *Nature 426*, 413−418] showed the presence of a unique heme, heme *x*, that is covalently linked by a single thioether bond to a Cys residue (Cys35) on the electrochemically negative (*n*) side of the cytochrome b_6 polypeptide. Heme *x* faces the intermonomer quinone exchange cavity. The only axial ligand associated with this heme is a H_2O or OH^- that is H-bonded to the propionate of the stromal side heme b_n, showing that it is pentacoordinate. The spectral properties of this heme were hardly defined at the time of the structure determination. The pyridine hemochromagen redox difference spectrum for heme *x* covalently bound to the cytochrome *b* polypeptide isolated from SDS−PAGE displays a low-amplitude broad spectrum with a peak at 553 nm, similar to that of other hemes with a single thioether linkage. The binding of CO and a hydrophobic cyanide analogue, butyl isocyanide, to dithionite-reduced b_6f complex perturbs and significantly shifts the redox difference visible spectrum. Together with EPR spectra displaying *g* values of the oxidized complex of 6.7 and 7.4, heme *x* is defined as a ferric high-spin heme in a rhombic environment. In addition to a possible function in photosystem I-linked cyclic electron transport, the five-coordinate state implies that there is at least one more function of heme *x* that is related to axial binding of a physiological ligand.

The X-ray structure of the cytochrome b_6f complex from the thermophilic cyanobacterium *Mastigocladus laminosus* (*1*) and the green alga *Chlamydomonas reinhardtii* (*2*) documented the presence of a heme, which was almost unrecognized in the previous literature, that is adjacent and approximately orthogonal to the *b*-type heme (b_n) on the electrochemically negative (*n*) side of the complex (Figure 1).[1] The unprecedented absence of any amino acid side chain in its axial coordination, and its covalent coordination to the protein by one thioether linkage, led to the designation of this heme as heme *x* (*1*) or, alternatively, c_i (*2*). The former notation will be used in this report. Heme *x* was found in the site occupied by the ubiquinone molecule bound on the *n*-side of the cytochrome bc_1 complex in the mitochondrial respiratory chain. The single covalent thioether bond involves a conserved cysteine residue (Cys35) on the *n*-side (stromal side) of helix A of the cytochrome b_6 subunit of the b_6f complex. Cys35 is not part of a signature heme binding sequence (-Cys-X-Y-Cys-His-) that is diagnostic for *c*-type hemes. Electron density in the b_n-proximal axial ligand position is consistent with ligation of heme *x* by a water or OH^- molecule that is hydrogen bonded to the carboxylate of the propionate side chain at position 7 of heme b_n and the backbone of the neighboring Gly38. However, no electron density has been resolved in the other axial position of heme *x* that contacts the intermonomer quinone exchange cavity. The absence of an amino acid axial ligand for heme *x*, together with its covalent attachment by only one thioether bond, confers on it properties of a unique heme prosthetic group.

Unlike the other *c*- and *b*-type cytochromes in the energy-transducing bc_1 and b_6f complexes, which were unequivocally detected by chemical and light minus dark difference spectrophotometry, heme *x* had not previously been detected prior to the structure analysis by most analyses using such methods, and therefore had not been recognized and is not included in almost all descriptions of the photosynthetic electron transport chain. An exception is a set of analyses on the green alga *Chlorella sorokinia* using flash kinetic spectroscopy (*3*, *4*). In these studies, the presence of an

[†] This research was supported by National Institutes of Health Grants GM-38323 (W.A.C.) and GM-61904 (M.K.B.) and U.S. Department of Energy Grant DE-FG03-98ER20299 (D.M.K.).

* To whom correspondence should be addressed. Telephone: (765) 494-2269. Fax: (765) 496-1189. E-mail: wac@bilbo.bio.purdue.edu or hzhang@bilbo.bio.purdue.edu.

[‡] Purdue University.

[§] Battelle Northwest Laboratory.

[||] Washington State University.

[1] Abbreviations: BIC, butyl isocyanide; E_{m7}, midpoint oxidation−reduction potential at pH 7; EPR, electron paramagnetic resonance; FeCN, ferricyanide; *n*- and *p*-side, membrane side with negative and positive electrochemical potential, respectively; NQNO, 2-*n*-nonyl-4-hydroxyquinoline *N*-oxide; PQ, plastoquinone; SDS−PAGE, sodium dodecyl sulfate−polyacrylamide electrophoresis; UDM, β-D-undecyl maltoside.

10.1021/bi048363p CCC: $27.50
Published on Web 12/04/2004

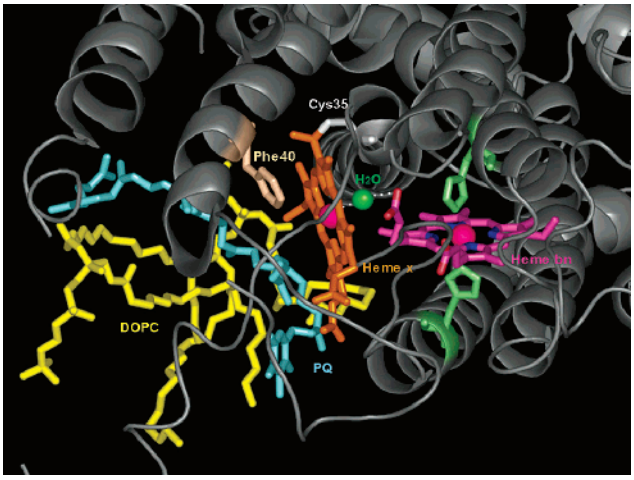

FIGURE 1: Heme *x* binding environment. View normal to the membrane plane from the stromal side: heme b_n, purple; His ligands for heme b_n, lime; heme *x*, orange; Cys35 thioether bound to heme *x*, white; Phe40 in subunit IV, wheat; PQ, cyan; lipid molecules (DOPC), yellow. The water or OH^- molecule that bridges heme b_n and *x* is displayed as a green ball; protein subunits are shown as gray ribbons.

additional electron transfer component in the b_6f complex, "G", with properties resembling those of a high-spin cytochrome *c*′, was inferred from difference spectra induced by a light flash, and the perturbation of these spectra by CO. These properties have a significant correspondence to those associated with heme *x* in this study.

Now that the presence of the additional heme in the cytochrome b_6f complex has been unequivocally demonstrated by an X-ray structure from both a cyanobacterium (*1*) and green alga (*2*), it is important to determine the spectral properties of this unique heme to obtain information about its ligation and oxidation state, which have implications for its function. In this study, visible and EPR spectra have been obtained of heme *x* in the cytochrome b_6f complex prepared from the thermophilic cyanobacterium *M. laminosus* and spinach chloroplasts. The cytochrome b_6f complex from both sources was shown in previous studies to be pure by mass spectroscopic analysis (*5*) and formation of crystals that diffract to high resolution (*1*, *6*).

MATERIALS AND METHODS

Purification of the Cytochrome b_6f Complex. The cytochrome b_6f complex from spinach chloroplasts and a thermophilic cyanobacterium, *M. laminosus*, was purified according to the method of Zhang *et al.* (*6*−*8*).

Absorbance Difference Spectra. Optical chemical difference spectra were measured using a Cary 3 UV−visible spectrophotometer with a bandwidth of 2 nm. The spectral peaks and bandwidths are accurate to ±0.5 nm.

SDS−*PAGE*. SDS−PAGE (15%) was carried out using a Laemmli system (*9*) with a 1 mm gel run under constant current (12 mA) conditions. Samples were prepared in 50 mM Tris-HCl (pH 8.0) containing 4 M urea, 2% SDS, 5% glycerol, and 2.5% mercaptoethanol and boiled for 2 min before being loaded on the gel.

Isolation of Subunits from the Gel. The top two pink bands in the SDS−PAGE gel (Figure 3A), corresponding to cytochromes *f* and b_6, respectively, were excised and soaked in a buffer containing 30 mM Tris-HCl (pH 7.5), 50 mM

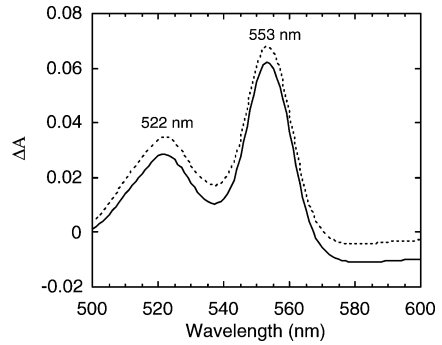

FIGURE 2: Pyridine hemochromagen difference (dithionite minus ferricyanide) spectrum of the complete cytochrome b_6f complex from *M. laminosus* (—) and spinach thylakoids (- - -).

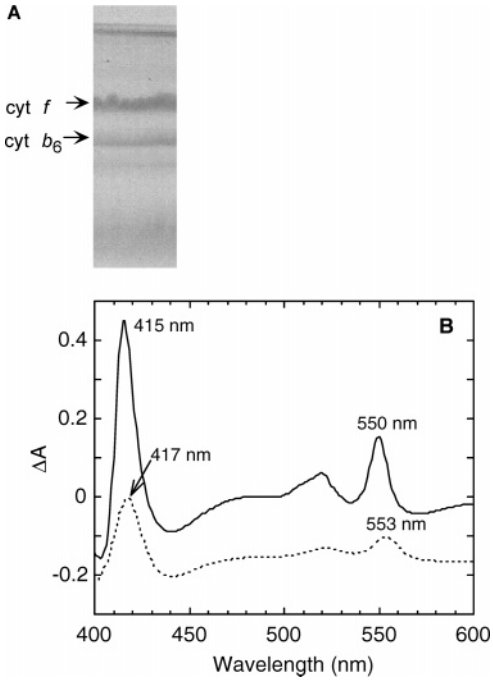

FIGURE 3: Pyridine hemochrome of extracted cytochrome *f* and cytochrome b_6 from SDS−PAGE. (A) SDS−PAGE of the isolated cytochrome b_6f complex from *M. laminosus*. (B) Spectra of pyridine hemochromes of cytochrome *f* (—) and b_6 (- - -) extracted from the gel.

NaCl, and 0.05% β-D-undecyl maltoside overnight or until the gel strips became colorless. The light pinkish "soaking solution" was collected for determination of pyridine hemochrome spectra of covalently bound hemes.

Determination of Pyridine Hemochrome Difference Spectra. Pyridine hemochromogen spectra were determined on the basis of the method of Berry *et al.* (*10*) with minor modifications. The cytochrome b_6f complex (600 μL, 1.5 mM) from *M. laminosus* or spinach chloroplasts was oxidized by addition of 1−2 grains of solid ferricyanide. Subsequently, 300 μL of pyridine and 100 μL of 1 N NaOH were added. After thorough mixing, the oxidized spectrum was recorded and used as a baseline for the difference spectrum. Solid dithionite (∼2−3 mg) was added, and the reduced minus oxidized difference spectrum was recorded.

Butyl Isocyanide and CO Difference Spectra. The cytochrome b_6f complex (1 mL, 1 μM) was reduced in a cuvette by an addition of an excess (∼2−3 mg) of solid dithionite. The cuvette was then sealed with Parafilm, and the sample was mixed by inverting the cuvette several times and

incubated for 10 min at room temperature. A series of baseline spectra were taken until there was no change in absorbance. Butyl isocyanide (BIC) (from Aldrich) was injected into the sealed cuvette to a final concentration of 10 mM, and a difference spectrum was recorded. For CO binding experiments, CO was delivered into the dithionite-reduced sample in a sealed cuvette for 2 min, and the difference spectrum was measured as described above.

EPR Spectroscopy. The cytochrome b_6 *f* complex from *M. laminosus* (15 μM) and spinach chloroplasts (17 μM) was prepared in the presence of ferricyanide (125 μM) or ascorbate (500 μM), and dithionite-reduced samples by adding ~2−3 mg of dithionite. Azide or cyanide was added to ferricyanide-oxidized or dithionite-reduced samples to a final concentration of 2.5 mM.

Electron paramagnetic resonance spectra at 20 K were obtained using a Bruker ESP300E system (Bruker Instruments, Billerica, MA). The EPR parameters were as follows: temperature of 20 K, microwave frequency of 9.44 GHz, microwave power of 20 mW, modulation amplitude of 20 G, gain of 1×10^5, and conversion time of 20 ms.

EPR spectra of the spinach b_6 *f* complex at 6 K were obtained using a Bruker 300 EPR spectrometer. The sample temperature was regulated using a GFS-300 transfer tube, an ESR-900 helium cryostat, and a model ITC4 temperature controller (Oxford Instruments, Oxford, U.K.). EPR parameters were as follows: temperature of 6 K, microwave frequency of 9.46 GHz, microwave power of 10 mW, modulation amplitude of 20 G, gain of 2×10^4, and conversion time of 40 ms. EPR spectra at 2.9 K were measured using a Bruker 380E spectrometer with a dielectric resonator immersed in liquid helium in a CFG-935 cryostat, with 1.56 kHz field modulation, and an amplitude of 10 G. The temperature was determined from the vapor pressure of the liquid helium.

RESULTS

Visible Absorbance Spectra of the Cytochrome b_6f Complex. Reduced minus oxidized chemical difference α-band spectra obtained at room temperature for the cytochrome b_6 *f* complex (*11*) show essentially a single spectral band at 563−564 nm with a half-bandwidth of approximately 10−11 nm, in addition to a band at 553−554 nm associated with cytochrome *f*. Spectra of the complex in intact membranes show similar α-band absorbance peaks for the two *b*-hemes, b_n and b_p, centered at 563−564 nm in thylakoids and cells (*4*, *12*, *13*). These spectra revealed no evidence for the presence of an additional spectral component that might be associated with heme *x*. Because of the spectral sharpening at low temperature, low-temperature difference spectroscopy is a more sensitive method for separating closely positioned spectral bands. Such spectra of the b_6 *f* complex from spinach thylakoids, measured at 77 K, exhibited three blue-shifted spectral components in the α-band region, at 557.5, 561.5, and 560.5 nm. The 560.5 nm band was assigned to the low-potential b_p, and the 557.5 and 561.5 nm peaks were ascribed to heme b_n based on their dependence on the ambient redox potential (*14*).

A search for heme *x* in difference spectra at 20 K was carried out. Dithionite minus ascorbate-reduced spectra were measured at 20 K, and first and second derivatives of the absorbance spectra were calculated to look for minor bands or "shoulders" in the spectra. Only two peaks were resolved, at 557 and 561 nm, in the absolute spectra and calculated second-derivative functions. Following Hurt and Hauska (*14*), these peaks were assigned, respectively, to a split spectrum of heme b_n and overlapping peaks of hemes b_n and b_p [n and p corresponding to h and l, respectively, in the notation of Hurt and Hauska (*14*)]. A search for the signature of heme *x* in the visible spectra of the isolated b_6 *f* complex was then carried out by analysis of the pyridine hemochromagen.

Spectra of Pyridine Hemochromes of the Cytochrome b_6 f Complex. There are apparently no previously published pyridine/hemochromagen spectra of the cytochrome b_6 *f* complex. Room-temperature chemical difference (dithionite minus ferricyanide) spectra of pyridine hemochromes of the b_6 *f* complex from *M. laminosus* (Figure 2, solid line) and spinach chloroplasts (Figure 2, dashed line) are virtually identical with an absorbance maximum at 553 nm and a half-bandwidth of 16 nm. These spectra contain overlapping contributions from one *c*-type heme (cytochrome *f*), two *b*-type hemes (b_p and b_n), and presumably heme *x*. The reported absorbance maximum of the cytochrome *f* pyridine hemochromagen is at 550 nm (*15*) and that of cytochrome *b* in the bc_1 complex at 556 nm (*10*) in more narrow spectra having half-bandwidths of 10.6 and 14.5 nm, respectively. The large extent of spectral overlap between the four heme components in the b_6 *f* complex, and the compression of their spectra, make it impossible to accurately resolve the spectra of the individual hemes in room-temperature pyridine hemochromagen difference spectra. A search for heme *x* in the isolated cytochrome b_6 polypeptide was then carried out.

Spectra of Pyridine Hemochromes of the Isolated Cytochrome f and b_6 Polypeptides. SDS−PAGE was used to separate the four large subunits in the cytochrome b_6 *f* complex. Covalently bound peroxidase-staining heme is retained on the gel in two positions, the cytochrome *f* polypeptide to which the heme is covalently bound and also at the position of the cytochrome b_6 polypeptide (*16*, *17*). The noncovalently bound *b*-type hemes were removed from the latter by the denaturing conditions in SDS−PAGE and are not seen on the gel (Figure 3A). Pyridine hemochromagen difference spectra were separately determined for the cytochrome *f* and b_6 polypeptides extracted from the gel. The extracted cytochrome *f* band shows a typical *c*-type pyridine hemochrome spectral peak at 550 nm with a half-bandwidth of 10.5 nm (Figure 3B, solid line) which, as expected, is identical to the spectrum of the cytochrome *f* pyridine hemochromagen from higher plants (*15*). However, the pyridine hemochrome spectrum of the heme chromophore attached to the cytochrome b_6 polypeptide shows a broad low-amplitude peak at 553 nm with a half-bandwidth of ~14.5 nm (Figure 3B, dashed line). The latter spectral peak is different from the reported value of hemochrome *b* that has an absorbance maximum at 556 nm (*10*), but it resembles that of other single-thioether bond *c*-type cytochromes from *Euglene gracilis* and *Crithidia oncopelti* (*18*). The spectral amplitude of the heme *x* pyridine hemochromagen is approximately 30% of that of cytochrome *f*, indicating a smaller extinction coefficient. The actual α-band peak in the native state of the high-spin heme *x*, which is not determined here, depends on the identity of the proximal heme ligand, whether it is H_2O or hydroxyl ion, the two possibilities that are

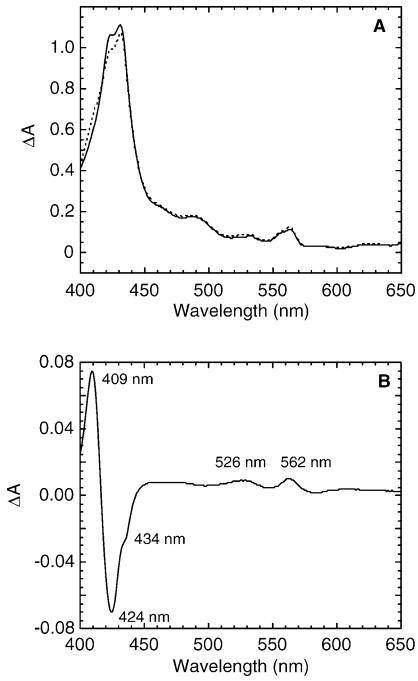

FIGURE 4: Visible spectra of CO derivatives of ferrous heme *x* in the cytochrome b_6f complex. (A) Dithionite-reduced spectra in the presence (- - -) and absence (—) of CO. (B) CO-reduced minus reduced difference spectrum.

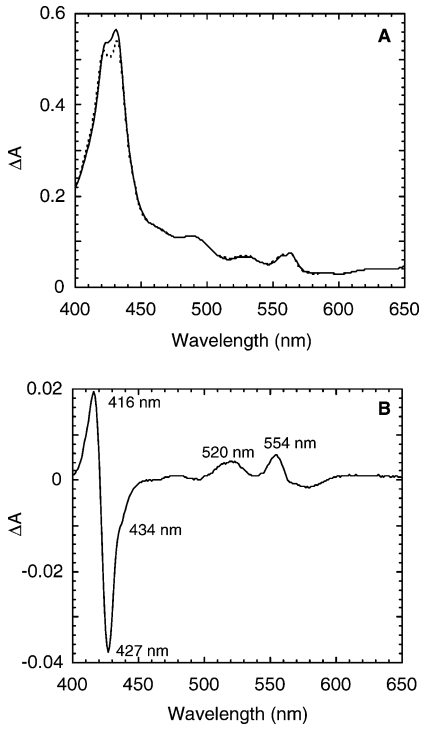

FIGURE 5: Visible spectra of BIC derivatives of ferrous heme *x* in the cytochrome b_6f complex. (A) Dithionite-reduced spectra in the presence (- - -) and absence (—) of BIC. (B) The BIC-reduced minus reduced difference spectrum, measured as described in Materials and Methods.

allowed from the X-ray structures of the cytochrome b_6f complex (*1*, *2*).

Derivatives of Heme x with Strong Field Ligands. A search in the visible spectra for the high-spin nature of heme *x* was carried out using small molecule strong field axial ligands that are expected to perturb the spectra of high-spin hemes. The addition of azide and cyanide had no effect on the visible spectra, perhaps because of their limited access to the heme in a hydrophobic environment. However, the addition of CO and butyl isocyanide caused a large perturbation and shift of the peaks of the visible absorbance spectrum. The CO difference spectrum of dithionite-reduced complexes from *M. laminosus* and spinach chloroplasts displayed a pronounced peak and trough in the Soret region around 409 and 424 nm, respectively, with a shoulder at 434 nm. Although it is not possible to precisely equate ligand-induced band shifts of isolated b_6f complex to the peaks of the light minus dark difference spectra previously measured in *C. sorokinia*, the major trough at 424 nm is similar to that seen in the difference spectrum attributed to component "G" observed by Lavergne (*3*) and Joliot and Joliot (*4*). This suggests that the redox component in the b_6f complex that binds CO is the component labeled G in those studies. An identification of the trough in the Soret band difference spectra (Figures 4B and 5B derived from Figures 4A and 5A) with the absorbance peak of heme *x* can be made because the band shifts (11−15 nm) in the difference spectra are similar to the width of the Soret band difference spectra. Two other broad peaks centered at 562 and 526 nm, along with a broad spectral trough centered at 583 nm, were also observed in both complexes (Figure 4B).

The difference spectrum in the presence, relative to the absence, of the BIC−b_6f complex exhibited two broad absorbance maxima centered at 554 and 520 nm, a peak and a trough at 416 and 427 nm, respectively, in the Soret region, and a shoulder at 434 nm (Figure 5B). This trough at 427 nm also resembles that seen in the studies on component G (*4*). Moreover, the shoulder on the trough at 434 nm is common to both the CO and BIC difference spectra (Figures 4B and 5B) and was seen in spectra of a cytochrome *c*′ (*19*). A broad spectral trough centered at 579 nm was also present in the difference spectrum. Butyl isocyanide has been used to perturb the spectra of high-spin myoglobin and hemoglobin (*20*), and the flavocytochrome *b* in neutrophil membranes (*21*). Spectral perturbation caused by butyl isocyanide was not observed on the purified yeast bc_1 complex under the same experimental conditions (data not shown). Together with the absence in the CO and BIC difference spectra of a trough at the Soret and α-band region (432 and 563 nm, respectively) of cyt b_6, it is inferred that the ligands do not bind significantly to the hemes of cytochrome b_6.

If an extinction coefficient of 26 mM^{-1} $heme^{-1}$ cm^{-1} for cytochrome b_6 is used for the spectral band at 563 nm, and if all of the heme *x* binds butyl isocyanide, then the extinction coefficient for the BIC−heme *x* complex at 554 nm would be 10.6 mM^{-1} $heme^{-1}$ cm^{-1} with half-bandwidths of 14 and 22 nm for α- and *β*-bands, respectively. As discussed above (first paragraph of the Results), heme *x* in the native state without any strong field ligand is almost invisible in the cytochrome α-band region in the background of the three other heme proteins in the complex. A small amplitude in the α−*β* region is a common feature of high-spin heme proteins (*19*, *22*).

EPR Spectra. EPR spectra of the cytochrome b_6f complex from *M. laminosus* and spinach chloroplasts were measured at 20 K (Figure 6A) and 6 K (Figure 6B). The principle *g* values at 7.3−7.4, 6.6−6.7, 6.0, 4.7, 4.3, and 3.5 can be seen at 20 K in the ferricyanide-oxidized (Figure 6A, traces

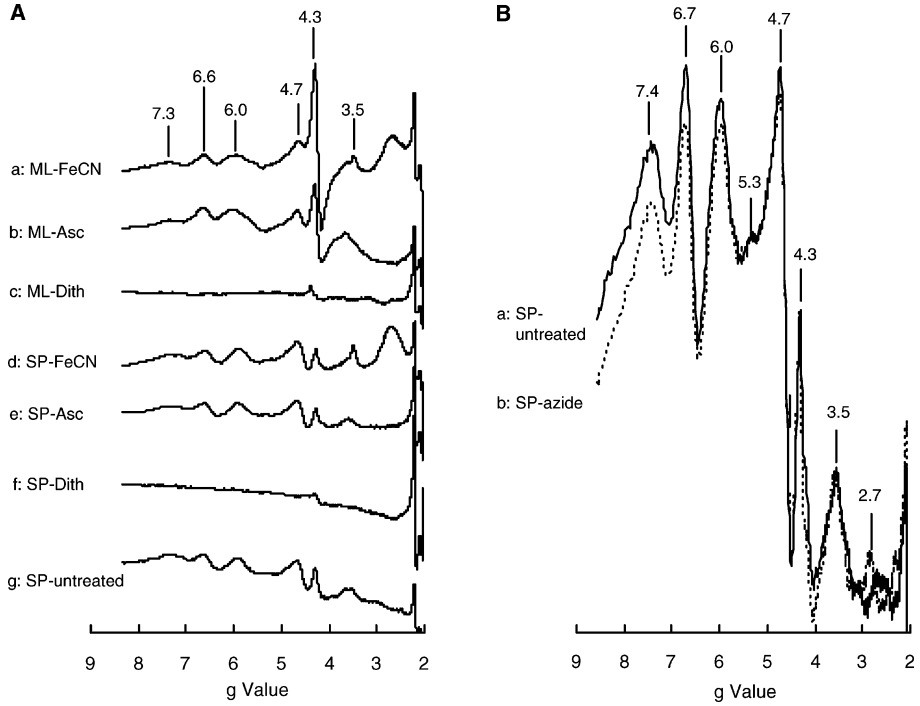

FIGURE 6: EPR spectra of (A) the cytochrome b_6f complex from *M. laminosus* and spinach thylakoid membranes at 20 K. Spectra from the *M. laminosus* complex in the presence of (a) ferricyanide (FeCN, 125 μM), (b) ascorbate (Asc, 400 μM), and (c) dithionite (~1 mM). Spectra of the spinach complex in the presence of (d) ferricyanide, (e) ascorbate, and (f) dithionite and (g) the untreated spinach complex. (B) Cytochrome b_6f complex from spinach chloroplasts (a) untreated and (b) with azide, measured at 6 K.

a and d), ascorbate-reduced (Figure 6A, traces b and e), and the untreated complex at 6 K (Figure 6B, trace a). The presence of the low field lines in the ascorbate-reduced samples implies that these lines originate from a redox component with an E_m of less than 50−100 mV, the operating potential of ascorbate. The larger amplitudes and smaller bandwidths of the 6 K spectra, shown most dramatically for the high-spin $g = 7.4$ signal, document qualitatively a large temperature dependence for the underlying transitions. The major spectral difference between the complex from *M. laminosus* (Figure 6A, traces a−c) and spinach (Figure 6A, traces d−g) at 20 K is the amplitude of the $g = 4.3$ signal, which arises from the first excited Kramer's doublet (*23*) that disappears at low temperatures (Figure 7).

The $g \sim 3.5$ signal in the ferricyanide-oxidized and the ascorbate-reduced complex mainly arises from the low-spin ferric hemes of cytochrome *f* and cytochrome b_6 (Figure 6A, traces a, b, d, and e). These *g* values and redox properties are consistent with those previously reported in EPR spectra of the cytochrome b_6f complex (*24*, *25*). The 6 K spectra confirm that there is no reactive site for azide in the complex (Figure 6B), consistent with the absence of an effect on the visible difference spectra as discussed above in the context of Figure 4.

The major EPR signals seen at *g* values of 7.3−7.4, 6.6−6.7, 6.0, and 4.7 (Figure 6A, traces a, b, d, e, and g; Figure 6B) fall into two groups based on temperature dependence and power saturation. A small presumably broadened signal is seen at $g = 5.3$ in the spectrum measured at 6 K (Figure 6B). The $g = 7.4$, 6.7, and 4.7 signals are saturates at a moderate microwave power at a low (~3 K) temperature, while the $g = 6.0$ signal does not. At 2.9 K, the amplitudes of all high-spin signals except the $g = 6.0$ signal are lost at a microwave power of 0.01 mW, but the $g = 6.0$ signal is much less affected (Figure 7). The different temperature dependence of the $g = 6.0$ band implies that it does not have the same origin as the other high-spin signals. The $g = 6.0$ component has previously been associated with heme signals from the denatured b_6f complex (*24*). In the case presented here, denatured cytochrome b_6 was not detected in the X-ray structure. It is possible that a small amount of the complex is denatured during sample freezing, and this component is excluded from the crystals. The spectra in Figure 6 imply the existence of two pairs of rhombic signals, $g = 7.4$ and 4.7 and $g = 6.7$ and 5.3, which correspond, respectively, to values of the rhombic distortion parameter,

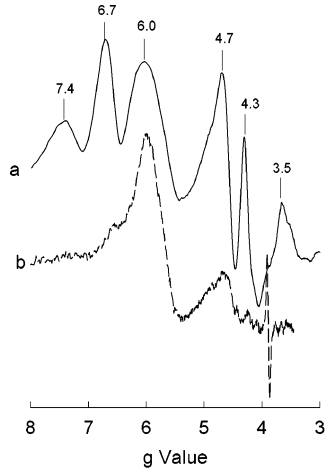

FIGURE 7: High-*g*-value EPR signals from the b_6f complex at 14 K (top trace) and 2.9 K (bottom trace). The sharp line near $g = 3.9$ in the bottom trace is from a Cr(III) impurity in the dielectric resonator. The microwave power was 0.01 mW for both spectra; modulations for traces a and b are 30 G at 100 kHz and 10 G at 1.56 kHz, respectively. The two spectra have been scaled so that they have comparable amplitudes.

E/*D* (*23*), of 0.058 and 0.029. It is hypothesized that the species with the more symmetrical, lower-rhombicity signal ($g = 6.7$ and 5.3) corresponds to the structure observed in the crystal structure. The broadening of the $g = 5.3$ signal is attributed to dipolar interactions (*26*) with a magnitude of 1−2 GHz from the nearby (9−10 Å Fe−Fe distance) heme b_n. Considering the high-spin *g* values in the spectra, there are four distinct species indicated by the spectra: the two rhombic pairs listed above, a $g = 6.0$ axial species, and a highly rhombic species giving rise to the $g = 4.3$ peak. The latter two might arise from denaturation. The second ($g = 7.4$ and 4.7) rhombic pair observed with the soluble complex could arise from a conformational change in or near heme *x*, which decreases the dipolar broadening and changes the zero-field splittings.

DISCUSSION

Accessibility of Heme x to Exogenous Ligands. The cavity side heme surface of heme *x* is surrounded by aromatic or other hydrophobic side chains. Phe40 and Leu37 in helix E of subunit IV, together with a bound plastoquinone and two lipid molecules, form a hydrophobic shield over the heme *x* surface, and the accessibility of exogenous ligands to the sixth coordination site of the Fe of heme *x* is limited. Thus, addition of cyanide and azide caused no change in the absorbance spectra, and they are assumed to be unreactive with heme *x*. This is a property of many high-spin cytochromes (*19*). In contrast, the small neutral molecule, CO, and a hydrophobic cyanide, butyl isocyanide, bind to the reduced heme *x* and perturb its visible spectrum. The visible spectral changes associated with the binding of BIC and CO are similar to those observed for the binding of EIC and CO to a cytochrome *c*′ from the photosynthetic bacterium *Rhodospirillum rubrum* (*27*). The spectral shifts caused by addition of CO or BIC are indicative of a high-spin−low-spin transition.

Redox Potential of Heme x. Spectral changes caused by the addition of butyl isocyanide and CO were observed only in the dithionite-reduced complex, not in ascorbate-reduced or ferricyanide-oxidized samples. It is known that CO can bind to only the reduced heme proteins (*19*). Therefore, it was inferred that the midpoint potential of the CO- and BIC-reactive component is less than that of the operating potential of ascorbate (approximately 50−100 mV). With regard to a more precise determination of the E_m, the available information is somewhat disparate. From the equilibrium between G and heme b_n in *C. sorokinia*, it was inferred that the midpoint potential of G is 20 mV more positive than that of heme b_n [E_m(G, heme *x*) > heme b_n], so E_m(heme *x*) ∼ −30 mV (*4*). This E_m is consistent with the presence of oxidized heme *x* as defined by the spectroscopic analysis in this study. An E_m of approximately −30 mV, together with the position of the bound plastoquinone observed within 3.1 Å of heme *x* in the *M. laminosus* structure (*1*), suggests an *n*-side electron transfer pathway involving heme *x*:

$$\text{heme } b_n(\text{red}) + \text{heme } x(\text{ox}) \rightarrow \text{heme } b_n(\text{ox}) + \text{heme } x(\text{red}) \quad (1)$$

$$\text{heme } x(\text{red}) + \text{PQ (or } PQ^{\bullet -} + 2H^+) \rightarrow \text{heme } x(\text{ox}) + PQ^{\bullet -} \text{ or } PQH_2 \quad (2)$$

This pathway and the position of PQ in the structure suggest that the mechanism of action of the quinone analogue inhibitor, NQNO, which is known to increase the amplitude of the flash-induced cytochrome *b* reduction (*28*), is to displace the PQ molecule in the intermonomer cavity.

On the other hand, consideration of other data in the literature in the context of the scheme described in reactions 1 and 2 implies a redox potential of heme *x* more reducing than that suggested in ref *4*. In particular, it has previously been observed that at a positive potential, where the PQ pool is fully oxidized, flash-induced turnover of PS II results in a large amplitude, and quite stable reduction of cyt b_n, even in the absence of Q_n site inhibitors (*29*, *30*). This would not be expected if heme *x* served as the efficient electron acceptor of heme b_n. Therefore, in contrast to the prediction of the reaction direction of eq 1, the working redox potential from functional assays would appear to yield the relation E_m(heme *x*) < E_m(heme b_n), i.e., E_m(heme *x*) < −50 mV, so that heme b_n could not readily reduce heme *x*. During the operation of the Q-cycle, electron transfer from cyt b_n to PQ might thus involve a transient, energetically uphill reduction of heme *x*.

All of the above estimates of the E_m of heme *x* are consistent with its existence in the oxidized ferric state under physiological ambient conditions, as are the pronounced $g \geq 6$ EPR signals that are a diagnostic signature for an oxidized ferric state of heme *x*. The inference that heme *x* in the ambient environment of the isolated b_6f complex is in a high-spin ferric state is not in agreement with the conclusion, derived from resonance Raman spectra, that heme *x* is reduced in the b_6f complex from *Ch. reinhardtii* (*31*). A reduced heme *x in vivo* would preclude the redox changes in *C. sorokinia* that were attributed to component G (*3*, *4*). It is unlikely that the oxidation state of heme *x* differs as a consequence of structural differences between the complex in *Ch. reinhartii* and *M. laminosus*, because the structure of the b_6f complex from the two sources is virtually identical in all major aspects (*1*, *2*). As noted in the resonance Raman study (*31*), photoreduction of the heme by the laser light used to excite the signals in the Raman spectrum may be an alternate explanation of the presence of a reduced heme *x* under the conditions of those experiments (*31*).

Function of Heme x: Significance of Its High-Spin Five-Coordinate State. It has previously been proposed that the function of heme *x*, which is not found in the cytochrome bc_1 complex, is related to the pathway of cyclic electron transport (*1*, *2*). Although the b_6f and bc_1 complexes have numerous identities and homologies in structure−function relationships, it has been suggested that the requirement of the cyclic pathway connected to the low-potential electron carriers, ferredoxin and FNR, may be a pathway that is unique to the b_6f complex (*1*, *2*, *12*, *32*, *33*), and suggests a role for heme *x* in this pathway. If heme *x* functions in cyclic electron transfer, acting as an acceptor of one electron from ferredoxin, or from FNR (*7*), and as a donor of one electron to plastoquinone or plastosemiquinone (eqs 1 and 2 above), the operation of the Q-cycle (*34*) would require the oxidative turnover of only one quinol on the *p*-side of the membrane to accomplish the two-electron reduction of a quinone on the *n*-side.

However, caution must be observed in assigning a role for heme *x* in cyclic electron flow, since the observed rate

of cytochrome *b* reduction by NADPH-ferredoxin shows a kinetic limitation (*12*, *35*, *36*), which implies regulation and control of this pathway that is not understood at present (*37*). Moreover, work on C3 plants suggests that electron transport is apparently inhibited by mutation of a Fd:PQ oxidoreductase and a NADPH:PQ oxidoreductase (*38*). This implies that the major physiological pathway for reduction of PQ from stromal reductants might not include the cyt b_6f complex (*39*).

The assignment of a function of heme *x* in a cyclic electron transport pathway, even if ultimately proven correct, would not answer all of the questions about its properties. The question of the functional significance of the five-coordinate high-spin state of heme *x* remains to be answered. The high-spin state implies that, in addition to its electron transfer function, heme *x* may have another function that is related to binding of a physiological ligand.

ACKNOWLEDGMENT

We thank B. Trumpower for the purified yeast cytochrome bc_1 complex, S. Savikhin, N. Dashdorj, and H. Kim for measurement of the 20 K spectra, and J. Yan, R. Taylor, G. Kurisu, and J. L. Smith for helpful discussions.

NOTE ADDED IN PROOF

An E_m = +75 mV for heme *x* was recently reported (Rappaport, F., Pierre, Y., Picot, D., and Lavergne, J., Proc. 13th Int. Cong. Photosyn., Montreal, Sept., 2004, Abstr. 7394), based on redox titrations of the *b*6*f* complex from *Ch. reinhardtii*, with the possibility noted that a more negative E_m could arise from electrostatic interactions with heme *b*n.

REFERENCES

1. Kurisu, G., Zhang, H., Smith, J. L., and Cramer, W. A. (2003) Structure of the cytochrome b_6f complex of oxygenic photosynthesis: Tuning the cavity, *Science 302*, 1009−1014.
2. Stroebel, D., Choquet, Y., Popot, J.-L., and Picot, D. (2003) An atypical heam in the cytochrome b_6f complex, *Nature 426*, 413−418.
3. Lavergne, J. (1983) Membrane potential-dependent reduction of cytochrome b_6 in an algal mutant lacking photosystem I centers, *Biochim. Biophys. Acta 725*, 25−33.
4. Joliot, P., and Joliot, A. (1988) The low-potential electron-transfer chain in the cytochrome *b/f* complex, *Biochim. Biophys. Acta 933*, 319−333.
5. Whitelegge, J. P., Zhang, H., Taylor, R., and Cramer, W. A. (2002) Full subunit coverage liquid chromatography electrospray-ionization mass spectrometry ($LCMS^+$) of an oligomeric membrane protein complex: The cytochrome b_6f complex from spinach and the cyanobacterium, *M. laminosus*, *Mol. Cell. Proteomics 1*, 816−827.
6. Zhang, H., Kurisu, G., Smith, J. L., and Cramer, W. A. (2003) A defined protein-detergent-lipid complex for crystallization of integral membrane proteins: The cytochrome b_6f complex of oxygenic photosynthesis, *Proc. Natl. Acad. Sci. U.S.A. 100*, 5160−5163.
7. Zhang, H., Whitelegge, J. P., and Cramer, W. A. (2001) Ferredoxin:$NADP^+$ oxidoreductase is a subunit of the chloroplast cytochrome b_6f complex, *J. Biol. Chem. 276*, 38159−38165.
8. Zhang, H., and Cramer, W. A. (2004) Purification and crystallization of the cytochrome b_6f complex in oxygenic photosynthesis, in *Photosynthesis Research Protocols* (Carpentier, R., Ed.) pp 67−78, Humana Press, Totowa, NJ.
9. Laemmli, U. K. (1970) Cleavage of structural proteins during the assembly of the head of bacteriophage T4, *Nature 227*, 680−685.
10. Berry, E. A., and Trumpower, B. L. (1987) Simultaneous determination of heme *a*, *b*, and *c* from pyridine hemochrome spectra, *Anal. Biochem. 161*, 1−15.
11. Bendall, D. S., Davenport, H. E., and Hill, R. (1971) Cytochrome components in chloroplasts of the higher plants, *Methods Enzymol. 23*, 327−344.
12. Furbacher, P. N., Girvin, M. E., and Cramer, W. A. (1989) On the question of interheme electron transfer in the chloroplast cytochrome b_6 *in situ*, *Biochemistry 28*, 8990−8998.
13. Kramer, D. M., and Crofts, A. R. (1994) Re-examination of the properties and function of the *b* cytochromes of the thylakoid cytochrome *bf* complex, *Biochim. Biophys. Acta 1184*, 193−201.
14. Hurt, E. C., and Hauska, G. (1983) Cytochrome b_6 from isolated cytochrome b_6f complexes: Evidence for two spectral forms with different midpoint potentials, *FEBS Lett. 153*, 413−418.
15. Metzger, S. U., Cramer, W. A., and Whitmarsh, J. (1997) Critical analysis of the extinction coefficient of chloroplast cytochrome f, *Biochim. Biophys. Acta 1319*, 233−241.
16. Hurt, E. C., and Hauska, G. (1981) A cytochrome f/b_6 complex of five polypeptides with plastoquinol-plastocyanin-oxidoreductase activity from spinach chloroplasts, *Eur. J. Biochem. 117*, 591−599.
17. Wynn, R. M., Bertsch, J., Bruce, B. D., and Malkin, R. (1988) Green algal cytochrome b_6f complexes: Isolation and characterization from *Dunaliella saline*, *Chlamydomonas reinhardtii* and *Scenedesmus obliquus*, *Biochim. Biophys. Acta 935*, 115−122.
18. Pettigrew, G. W., Leaver, J. L., Meyer, T. E., and Ryle, A. P. (1975) Purification, properties and amino acid sequence of atypical cytochrome *c* from two protozoa, *Euglena gracilis* and *Crithidia oncopelti*, *Biochem. J. 147*, 291−302.
19. Bartsch, R. G. (1977) Cytochromes, in *The Photosynthetic Bacteria* (Clayton, R. K., and Sistrom, W. R., Eds.) pp 265−266, Plenum Press, New York.
20. Antonini, E., and Brunori, M. (1971) Hemoglobin and Myoglobin in their Reactions with Ligands, in *Frontiers in Biology* (Neuberger, A., and Tatum, E. L., Eds.) pp 13−39, North-Holland Publishing Co., Amsterdam.
21. Cross, A. R., Parkinson, J. F., and Jones, T. G. (1984) The superoxide-generating oxidase of leucocytes: NADPH-dependent reduction of flavin and cytochrome *b* in solubilized preparations, *Biochem. J. 223*, 337−344.
22. Meyer, T. E., and Kamen, M. D. (1982) New perspectives on *c*-type cytochromes, in *Advances in Protein Chemistry* (Anfinsen, C. B., Edsall, J. T., and Richards, F. M., Eds.) pp 105−212, Academic Press, New York.
23. Palmer, G. (1979) Electron paramagnetic resonance of hemeproteins, in *The Phorphyrins* (Dolphin, D., Ed.) pp 313−353, Academic Press, New York.
24. Nitschke, W., and Hauska, G. (1987) On the nature of the $g = 6$ EPR signal in isolated cytochrome b_6f complex from spinach chloroplasts, *Biochim. Biophys. Acta 892*, 314−319.
25. Nitschke, W., and Hauska, G. (1987) An asymmetric low-spin signal of cytochrome b_6 in the cytochrome b_6f complex from spinach chloroplasts, *FEBS Lett. 213*, 453−455.
26. Wilson, D. F., and Leigh, J. S. J. (1972) Heme-heme interaction in cytochrome *c* oxidase in situ as measured by EPR spectroscopy, *Arch. Biochem. Biophys. 150*, 154−163.
27. Rubinow, S. C., and Kassner, R. J. (1984) Cytochrome *c′* in their reaction with ethyl isocyanide, *Biochemistry 23*, 2590−2595.
28. Selak, M. A., and Whitmarsh, J. (1982) Kinetics of the electrogenic step and cytochrome b_6 and *f* redox changes in chloroplasts, *FEBS Lett. 150*, 286−292.
29. Kramer, D., and Crofts, A. R. (1993) The concerted reduction of the high and low potential chain of the *bf* complex by plastocyanin, *Biochim. Biophys. Acta 1183*, 72−84.
30. Kramer, D. M., and Crofts, A. R. (1992) A Q cycle type model for turnover of the *bf* complex under a wide range of redox conditions, in *Research in Photosynthesis* (Murata, N., Ed.) pp 491−494, Kluwer Scientific Publishers, Dordrecht, The Netherlands.
31. de Vitry, C., Desbois, A., Redeker, V., Zito, F., and Wollman, F.-A. (2004) Biochemical and spectroscopic characterization of the covalent binding of heme to cytochrome b_6, *Biochemistry 43*, 3956−3968.
32. Joliot, P., and Joliot, A. (2002) Cyclic electron transfer in plant leaf, *Proc. Nat. Acad. Sci. U.S.A. 99*, 10209−10214.

33. Finazzi, G., Rappaport, F., Furia, A., Fleischmann, M., Rochaix, J.-D., Zito, F., and Forti, G. (2002) Involvement of state transitions in the switch between linear and cyclic electron flow in *Chlamydomonas reinhardtii*, *EMBO J. 3*, 280−285.
34. Mitchell, P. (1975) The proton-motive Q cycle: A general formulation, *FEBS Lett. 59*, 137−139.
35. Kramer, D. M., and Crofts, A. R. (1990) A Q-cycle mechanism for electron transfer in chloroplasts, in *Current Research in Photosynthesis* (Baltscheffsky, H., Ed.) pp 283−286, Kluwer Academic Publishers, Dordrecht, The Netherlands.
36. Kramer, D. M. (1990) Ph.D. Thesis, Department of Physiology and Biophysics, University of Illinois, Urbana, IL.
37. Kramer, D. M., Avenson, T. J., and Edwards, G. E. (2004) Dynamic flexibility in the light reactions of photosynthesis governed by both electron and proton transfer reactions, *Trends Plant Sci. 9*, 349−357.
38. Munekage, Y., Hashimoto, M., Miyake, C., Tomizawa, K., Endo, T., Tasaka, M., and Shikanai, T. (2004) Cyclic electron flow around photosystem I is essential for photosynthesis, *Nature 429*, 579−582.
39. Bendall, D. S., and Manasse, R. S. (1995) Cyclic phosphorylation and electron transport, *Biochim. Biophys. Acta 1229*, 23−38.

BI048363P